

## RESEARCH ARTICLE

10.1002/2015JG003057

## Key Points:

- High-resolution mapping of nitrogen reduction pathways within Niantic River
- Sulfide concentration was the best predictor of nitrogen reduction pathway
- Organic carbon quality was more important than quantity

## Correspondence to:

P. Plummer,  
Patrick.t.plummer@uscga.edu

## Citation:

Plummer, P., C. Tobias, and D. Cady (2015), Nitrogen reduction pathways in estuarine sediments: Influences of organic carbon and sulfide, *J. Geophys. Res. Biogeosci.*, 120, doi:10.1002/2015JG003057.

Received 15 MAY 2015

Accepted 15 SEP 2015

Accepted article online 21 SEP 2015

## Nitrogen reduction pathways in estuarine sediments: Influences of organic carbon and sulfide

Patrick Plummer<sup>1</sup>, Craig Tobias<sup>2</sup>, and David Cady<sup>2</sup>

<sup>1</sup>Department of Science, United States Coast Guard Academy, New London, Connecticut, USA, <sup>2</sup>Department of Marine Sciences, University of Connecticut, Groton, Connecticut, USA

**Abstract** Potential rates of sediment denitrification, anaerobic ammonium oxidation (anammox), and dissimilatory nitrate reduction to ammonium (DNRA) were mapped across the entire Niantic River Estuary, CT, USA, at 100–200 m scale resolution consisting of 60 stations. On the estuary scale, denitrification accounted for ~90% of the nitrogen reduction, followed by DNRA and anammox. However, the relative importance of these reactions to each other was not evenly distributed through the estuary. A Nitrogen Retention Index (NIRI) was calculated from the rate data (DNRA/(denitrification + anammox)) as a metric to assess the relative amounts of reactive nitrogen being recycled versus retained in the sediments following reduction. The distribution of rates and accompanying sediment geochemical analytes suggested variable controls on specific reactions, and on the NIRI, depending on position in the estuary and that these controls were linked to organic carbon abundance, organic carbon source, and pore water sulfide concentration. The relationship between NIRI and organic carbon abundance was dependent on organic carbon source. Sulfide proved the single best predictor of NIRI, accounting for 44% of its observed variance throughout the whole estuary. We suggest that as a single metric, sulfide may have utility as a proxy for gauging the distribution of denitrification, anammox, and DNRA.

### 1. Introduction

Estuarine denitrification and anaerobic ammonium oxidation (anammox) export reactive nitrogen from marine ecosystems back to the atmosphere, while dissimilatory nitrate/nitrite reduction to ammonium (DNRA) conserves reactive nitrogen within the ecosystem. The magnitudes of these reduction pathways relative to the N loading provide some biogeochemical constraints on ecosystems susceptibility and resilience to excess nitrogen loading [Giblin *et al.*, 2013]. Denitrification in estuarine systems can be the dominant mechanism for nitrogen reduction, and therefore N removal [Cornwell *et al.*, 1999; Seitzinger *et al.*, 2006]. In carbon-rich environments denitrification rates are primarily controlled by  $\text{NO}_{3+2}^-$  availability which can be delivered from adjacent watersheds or produced in situ from nitrification [Kana *et al.*, 1998; Nielsen *et al.*, 1995]. In carbon-poor environments denitrification can be limited by organic carbon (OC) quantity [Caffrey *et al.*, 1993], and carbon quality provides an additional constraint on denitrification rates regardless of total OC abundance [Fulweiler *et al.*, 2007; Eyre and Ferguson, 2009; Tobias *et al.*, 2001]. Sulfate reduction can influence denitrification either by competing for electrons or through sulfide effects on specific enzymes involved in the multistep denitrification pathway. The final reduction step of denitrification of  $\text{N}_2\text{O}$  to  $\text{N}_2$  gas [Sørensen, 1987] can be inhibited by sulfide as can nitrification that would otherwise fuel coupled nitrification denitrification [Joye and Hollibaugh, 1995].

Unlike denitrifiers, anammox bacteria use ammonium ( $\text{NH}_4^+$ ) to reduce  $\text{NO}_2^-$  to yield  $\text{N}_2$  [Dalsgaard *et al.*, 2005]. There is no direct OC source of electrons required for the reduction, and there is no nitrous oxide intermediate during  $\text{N}_2$  production [Dalsgaard *et al.*, 2005]. Anammox may account for 30–50% of the total  $\text{N}_2$  removal from the ocean nitrogen budget [Devol, 2003; Engström *et al.*, 2009; Glud *et al.*, 2009; Kuypers *et al.*, 2005]. Although typically low, potential anammox rates within coastal sediments have been reported between 0 and  $52 \mu\text{mol N m}^{-2} \text{h}^{-1}$  [Brin *et al.*, 2014; Crowe *et al.*, 2012; Dalsgaard *et al.*, 2005; Meyer *et al.*, 2005]. The  $\text{NH}_4^+$  for the anammox reaction is supplied by various respiratory and/or dissimilatory pathways such as aerobic respiration, sulfate reduction, and DNRA [An and Gardner, 2002; Brandes *et al.*, 2007].  $\text{NO}_2^-$  can be supplied via  $\text{NO}_{3+2}^-$  reduction during denitrification, DNRA, or from aerobic ammonium oxidation [Trimmer *et al.*, 2005]. Little is known regarding the geochemical controls of anammox [Lisa *et al.*, 2014]. Denitrifiers are thought to outcompete anammox under conditions of high OC [Jin *et al.*, 2012], but there

are reports of enhanced anammox coincident with higher organic matter and the resultant increase  $\text{NH}_4^+$  supply from high organic matter mineralization rates [Meyer et al., 2005; Trimmer et al., 2003]. The reported effects of sulfate reduction on anammox range from sulfide inhibition [Dalsgaard et al., 2003; Jensen et al., 2008] to enhancement of rates by high sulfide [Wenk et al., 2013], to partial reliance of anammox on  $\text{NH}_4^+$  produced from sulfate reduction [Canfield et al., 2010].

DNRA retains N and can rival denitrification rates in many coastal, estuarine environments [Burgin and Hamilton, 2007; Dong et al., 2011; Giblin et al., 2013]. DNRA can proceed through either a heterotrophic (fermentation) or chemoautotrophic metabolic pathway [Giblin et al., 2013; King and Nedwell, 1985; Tiedje, 1988]. Low molecular weight OC sources serve as the electron donor for fermentative DNRA, while the chemoautotrophic metabolism uses inorganic substrates (e.g., sulfide) as a reductant [Tugtas and Pavlostathis, 2007]. DNRA requires three more electrons per mole of  $\text{NO}_3^-$  reduced than denitrification; therefore, DNRA may be a more important reduction pathway in strongly reducing environments replete with electrons [Mohan and Cole, 2007]. DNRA rates are linked to OC availability and quality [Tobias et al., 2001], the ratio of OC to nitrate [Algar and Vallino, 2014], and sulfide. High sulfide increases DNRA rates [Burgin and Hamilton, 2008; Gardner et al., 2006], but it remains unclear whether such observed enhancements of DNRA reflects sulfide inhibition of denitrification [Brunet and Garcia-Gil, 1996; Senga et al., 2006] or use of sulfide directly as an electron source, or both [An and Gardner, 2002].

Recent experimental and modeling efforts [Algar and Vallino, 2014; Kraft et al., 2014a] using labile carbon substrates suggest that the  $\text{OC:NO}_{3+2}^-$  is a reasonable predictor of Dissolved Inorganic Nitrogen (DIN) partitioning through denitrification, DNRA, and anammox, whereby anammox dominates at low ratios and DNRA dominates at the highest  $\text{OC:NO}_{3+2}^-$  ratios. Separate experiments with coastal sediments and water from oxygen minimum zones showed that the partitioning between denitrification and anammox was independent of organic matter (OM) load but instead depended most on the C:N ratio (i.e., amino acid content) of the OM [Babbin and Ward, 2013; Babbin et al., 2014]. The modeling and experimental work represent important steps toward understanding controls on DIN removal and recycling, but conclusions from these studies are difficult to extrapolate to the in situ conditions of coastal sediments for three reasons: (1)  $\text{NO}_{3+2}^-$  is rapidly consumed, and concentrations do not often reflect its load or availability; (2) coastal sediments are composed of a variety of carbon sources of different quality relative to model carbon substrates; and (3) sulfate reduction can directly or indirectly exert further selective controls on these reactions through competition for carbon, supply of substrates (e.g.,  $\text{NH}_4^+$  for anammox), and/or the production of sulfide that inhibits some pathways (e.g., denitrification) and not others.

The objectives of this study were twofold: first to characterize at a high spatial resolution the distribution of denitrification, anammox, and DNRA in a euryhaline temperate estuary using potential rates and second to relate spatial differences in potential N-cycling rates to the distribution of OC abundance, sulfate reduction (using pore water sulfide as a proxy), and bulk organic matter characteristics indicative of different carbon sources.

## 2. Methods

### 2.1. Site Description

The Niantic River Estuary (NRE) is a shallow estuary located in southeastern Connecticut ( $41^\circ 20' \text{N}$ ,  $072^\circ 11' \text{W}$ ), along the northern shore of Long Island Sound, USA (Figure 1). The watershed for the NRE covers over  $80 \text{ km}^2$ . The estuary is shallow (2–5 m) and tidally dominated, with semidiurnal tidal range of  $\sim 1 \text{ m}$ . The estuary receives nominal freshwater inputs at base flow, and salinity was uniformly high throughout the study period. The NRE consists of geomorphologically distinct areas including two upper branches, the lower estuary, and one protected cove (Smith Cove). The upper and lower estuary is separated by a sandbar that is exposed at low tide (Figure 1). Additionally, a large sea grass bed (*Zostera marina*) occupies the middle estuary, although it exhibited extensive dieback prior to sampling (Figure 1).

### 2.2. Field Sampling

Sixty sampling locations were selected in a  $0.4 \text{ km}$  long by  $0.2 \text{ km}$  wide, evenly spaced grid encompassing the entire estuary. At each location, water column and sediment samples were collected. Sampling was conducted over a 3 week period in August 2012. Bottom water measurements ( $0.5 \text{ m}$  above the sediment) made



**Figure 1.** Sampling locations within the Niantic River Estuary. The oval represents the approximate extent of sea grassbeds. The straight line marks the location of the sandbar that divides the “upper” and “lower” estuaries.

in the field consisted of pH, salinity, dissolved oxygen, specific conductivity, and temperature using a YSI 556 sonde (YSI Inc., Yellow Springs, Ohio, USA). Bottom water samples were collected for the following parameters:  $\text{NO}_3^-$ ,  $\text{NO}_2^-$ ,  $\text{NH}_4^+$  (DIN), particulate organic nitrogen and particulate organic carbon (PON, POC) concentrations,  $\delta^{15}\text{N}$ -PON, and  $\delta^{13}\text{C}$ -POC. DIN samples were field-filtered  $0.45\ \mu\text{m}$ . Particulate Organic Matter (POM) was captured on precombusted  $25\ \text{mm}$ ,  $0.7\ \mu\text{m}$ , glass microfibre filters. Both DIN samples and POM filters were stored on dry ice in the field. A pole corer was used to collect  $7.6\ \text{cm}$  diameter sediment cores. Surface sediments were sectioned (either 0–1, 1–2, 2–3, or 0–3 cm depending on analyses) in the field and divided into aliquots for N-cycling rate measurements and geochemical analyses. All sediments except a fraction for sediment chlorophyll *a* were packed in a headspace free container and iced in the field. Sediment to be used for chlorophyll *a* analysis was stored on dry ice in the dark after collection.

### 2.3. Geochemical Analysis

For the water column, PON and POC concentrations,  $\delta^{15}\text{N}$  and  $\delta^{13}\text{C}$  of the POM trapped on the filters were analyzed in duplicate using an elemental analyzer-isotope ratio mass spectrometer (EA-IRMS) following acidification to remove carbonates. Water column  $\text{NH}_4^+$ ,  $\text{NO}_3^-$ , and  $\text{NO}_2^-$  were measured using indophenol and Cd reduction/Azo dye methods, respectively, [Smith and Bogren, 2001; Solorzano, 1969] using a SmartChem analyzer. Precision on the isotope values was  $\pm 0.2\text{‰}$ . Detection limits and precision on duplicate field samples for the DIN analyses (surface and pore waters) were  $0.5\ \mu\text{M}$  and  $\pm 1\ \mu\text{M}$ , respectively.

The following analyses were conducted on bulk sediments and analyzed in duplicate: density, porosity, chlorophyll *a*, phaeopigments, C and N content,  $\delta^{15}\text{N}$  and  $\delta^{13}\text{C}$ , and extractable  $\text{NH}_4^+$ . The C and N content and stable isotopes were measured via EA-IRMS on freeze-dried sediments following acidification ( $^{15}\text{N}$  analyses were done on unacidified aliquots). Sediment chlorophyll *a* and phaeopigments were extracted in 100% acetone and quantified spectrophotometrically [Aminot and Rey, 2000]. Extractable  $\text{NH}_4^+$  adsorbed to sediment was desorbed by KCl extraction (1:2, sediment:2N-KCL) and measured using the indophenol blue method [Solorzano, 1969]. Pore waters were analyzed for ferrous iron, sulfide,  $\text{NH}_4^+$ ,  $\text{NO}_3^-$ , and  $\text{NO}_2^-$ . Pore water was separated by centrifugation under argon headspace,  $0.45\ \mu\text{m}$  filtered, and analyzed for  $\text{NH}_4^+$ ,  $\text{NO}_3^-$ , and  $\text{NO}_2^-$  using the methods described above. Pore water sulfide concentrations were analyzed using the methylene blue method [Cline, 1969]. Iron concentrations were analyzed using the ferrozine method [Stookey, 1970]. The detection limit and precision on the sulfide and ferrous iron analyses were  $1\ \mu\text{M}$  and  $2\text{--}3\ \mu\text{M}$ .

### 2.4. Sediment Incubations for N-Cycling Rates

Potential rates of denitrification and anammox and DNRA were measured using labeled  $^{15}\text{NO}_2^-$  tracer added to anaerobic sediment slurries outlined by Song and Tobias [2011] and Thamdrup and Dalsgaard [2002]. Sediment slurries of the top 0–2 cm were incubated in the dark under anaerobic conditions (ultrahigh purity He flushed in 12 mL Exetainers) for 24 h to remove all  $\text{NO}_{3+2}^-$ . A subset of the slurry samples were analyzed

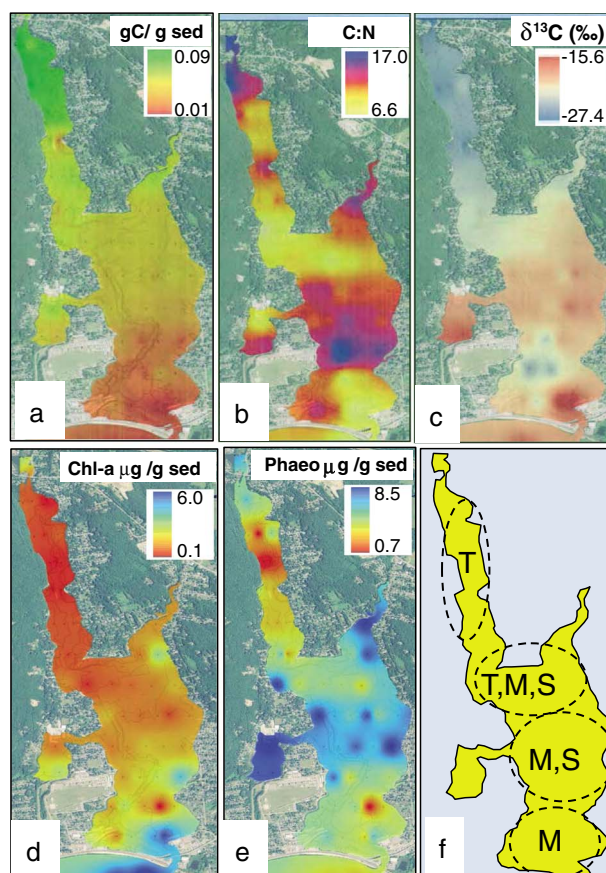


**Figure 2.** (a–e) Bulk OM characteristics were mapped using the same 60-point grid as the rate maps presented in Figure 1. (f) The study site is characterized by four zones of sediment OM type reflecting different contributions from terrestrial (T), microalgal (M; phytoplankton upstream and benthic microalgal downstream), and sea grass (S) sources.

of  $^{30}\text{N}_2$  and  $^{29}\text{N}_2$  results with respect to denitrification and anammox. Following gas analyses, the sediment slurries were extracted for  $\text{NH}_4^+$  by the addition of KCl. The  $\text{NH}_4^+$  was isolated from the extract by alkaline acid-trap diffusion and analyzed for  $^{15}\text{N}$  via EA-IRMS [Holmes *et al.*, 1998]. DNRA rates were calculated from the mass of  $^{15}\text{N}$  in the extracted  $\text{NH}_4^+$  produced during the incubation and the mole fraction enrichment of the  $^{15}\text{NO}_2^-$  addition.

### 3. Results

#### 3.1. Estuarine Geochemistry

During the sampling period, watershed discharge was low and the entire estuary was euhaline (27–30 practical salinity unit). DIN was low throughout the NRE and the dominant form,  $\text{NO}_{3+2}^-$ , never exceeded  $3\ \mu\text{M}$ . Bulk sediment physical properties exhibited an estuarine gradient in porosity and density with higher porosity and lower density occurring upstream. Similarly, sediment OC and organic nitrogen followed a gradient that increased with distance upstream likely reflecting increasing terrestrial organic matter contributions in the upper NRE (Figure 2a). The C:N ratios as well as other sediment/pore water parameters revealed more of a patchwork distribution in geochemistry rather than clear gradients. The C:N,  $\delta^{13}\text{C}$ , chlorophyll *a*, and phaeopigments showed zonal differences between the northwestern (NW) and northeastern (NE) upstream branches, the grassbed centrally located in the NRE, and in the sediments located seaward of the grassbed (Figures 2a–2f). Sediment C:N throughout the whole NRE varied from 6.6 to 17 but was heterogeneously distributed (Figure 2b). Higher C:N ratios found in the upper branches of the NRE indicated higher terrestrial

for  $\text{NO}_3^-$  and  $\text{NO}_2^-$  using chemiluminescent vanadium reduction to  $\text{NO}$  [Braman and Hendrix, 1989] to account for any residual  $\text{NO}_{3+2}^-$  prior to tracer addition. Slurries were then He purged for a second time, and  $^{14}\text{NH}_4^+ + ^{15}\text{NO}_2^-$  (99.9 at. %  $^{15}\text{N}$ ) were added to the incubations to a final pore water concentration of  $55\ \mu\text{M}$  each. Nitrite tracer was chosen instead of nitrate tracer because it permitted the uncoupling of nitrite availability (e.g., for anammox) from the  $\text{NO}_3^-$  to  $\text{NO}_2^-$  reduction step in denitrification. Time series incubation samples were analyzed in real time, and denitrification and anammox rates were calculated from linear regressions of  $^{30}\text{N}_2$  and  $^{29}\text{N}_2$  production, respectively, [Thamdrup and Dalsgaard, 2002] as measured with gas chromatography IRMS at 36 min intervals from 0 to 252 min. Rates were corrected using adjusted  $^{15}\text{NO}_2^-$  enrichment-based  $\text{NO}_{3+2}^-$  measured in the subset of slurry samples and were typically less than a 5% adjustment in the calculated rates. Root-mean-square error on the rates derived from the regressions was on the order of 10–20% for both the anammox and denitrification rates. Parallel incubations were conducted with  $^{15}\text{NH}_4^+$  only to verify the absence of coupled nitrification/denitrification, which would have affected interpreta-

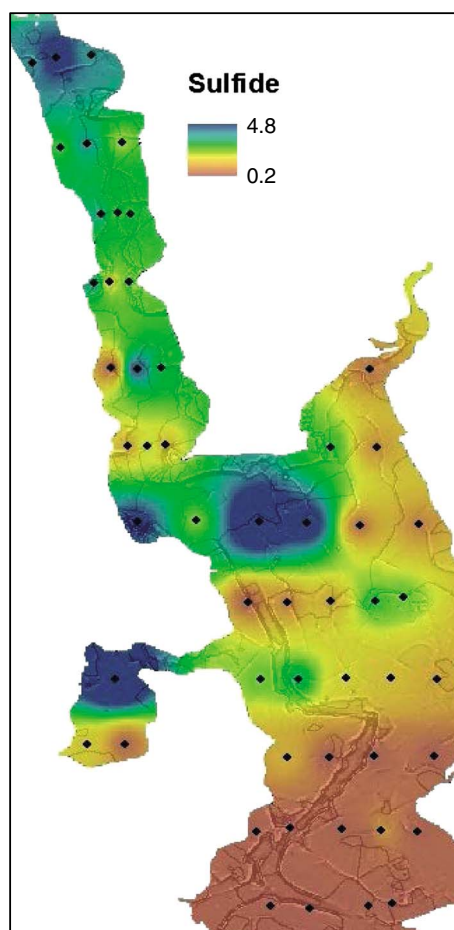


**Figure 3.** NRE pore water sulfide distribution (millimolar).

distance upstream with the exception of the NE branch that showed elevated chlorophyll *a* (and phaeopigments) relative to the upper NW branch. Phaeopigment concentrations (0–1 cm deep) ranged from 0.7 to 8.5  $\mu\text{g}$  pheao  $\text{g}$  sediment<sup>-1</sup> (Figure 2d). Phaeopigments, indicative of degrading photosynthetic organic matter, showed marked increase in grassbeds that recently died off. Phaeopigments were absent from the NW upper branch, but not the NE branch of the NRE. Smith Cove also showed high phaeopigments resulting from high macroalgal and microalgal turnover characteristic of this long residence time water mass.

In the pore waters, nitrate was below detection at all stations, but 11 stations contained pore water nitrite with 8 stations ranging from 1 to 3  $\mu\text{M}$ , while 3 stations exceeded 10  $\mu\text{M}$ . All stations contained measurable extractable ammonium ranging from 22 to 510  $\mu\text{M}$ ; however, neither ammonium nor nitrite was correlated with upstream-downstream position in the estuary but instead reflected local organic matter abundance. Sulfide concentrations ranged from 0.2 to 4.8 mM throughout the estuary and were generally higher in the upper estuary although there was variation throughout the NRE (Figure 3). Sulfide was weakly correlated with OC with the broadest range of sulfide concentrations (0 to >3.5 mM) occurring across stations of intermediate OC content (0.02–0.04  $\text{gC}$   $\text{g}$  sediment<sup>-1</sup>; Figure 4). Sulfide hot spots occurred in the uppermost NW branch, upper central NRE, and in Smith Cove but were notably low along the whole eastern edge of the NRE from top to bottom (Figure 3). Ferrous iron was detectable (0.2 to 127  $\mu\text{M}$ ) at only 15 of the 60 stations tested and was limited to locations within the estuary where sulfide was < 1 mM.

### 3.2. Nitrogen Reduction Reactions

#### 3.2.1. Denitrification

Observed rates of denitrification ranged from 0 to 75  $\mu\text{mol N m}^{-2} \text{h}^{-1}$  for the NRE with the highest rate measured in Smith Cove (Figure 5a). The maximum rate for the remainder of the estuary was 62  $\mu\text{mol N m}^{-2} \text{h}^{-1}$ .

inputs, but there was also elevated C:N ratio within and near the location of the sea grass beds. All other locations (seaward of the grassbed and at the base of the NW branch) showed lower C:N ratios more consistent with microalgal inputs. The  $\delta^{13}\text{C}$  generally increased from a minimum of  $-27.4\text{‰}$  near the head of the estuary a maximum of  $-15.6\text{‰}$  at the mouth of the estuary, with moderately heavy values persisting in the NE branch of the NRE relative to the NW branch (Figure 2c). Based upon the range of  $\delta^{13}\text{C}$  and position in the estuary, low  $\delta^{13}\text{C}$  values (<  $-21\text{‰}$ ) were interpreted as indicative of terrestrial carbon inputs. The most enriched  $\delta^{13}\text{C}$  values ( $\sim 15\text{--}16\text{‰}$ ) in the lower NRE were coincident with coarse sediments and dense benthic microalgal communities. Intermediate  $\delta^{13}\text{C}$  values ( $\sim 17\text{--}21\text{‰}$ ) were interpreted as OC derived from estuarine phytoplankton [Bianchi and Canuel, 2011]. Sediment chlorophyll *a* (0–1 cm deep) ranged from 0.1 to 6.0  $\mu\text{g}$  chlorophyll *a*  $\text{g}$  sediment<sup>-1</sup> (Figure 2d). The maximum sediment chlorophyll *a* concentrations were measured at the mouth of the estuary likely reflecting phytodetritus and benthic microalgae. Chlorophyll *a* decreased with

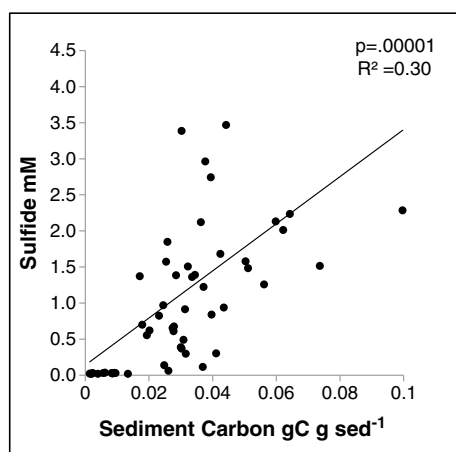


**Figure 4.** Linear regression of pore water sulfide as a function of sediment organic carbon content—all stations.

$3.1 \mu\text{mol N m}^{-2} \text{h}^{-1}$ . Anammox and denitrification were tightly correlated throughout the estuary ( $r^2 = 0.81$ ,  $p < 0.001$ ), although a notable exception was the NE branch of the upper NRE where denitrification was high but anammox was low. The ratio of anammox to denitrification ( $^A/D$ ) was small and ranged from 0.01 to 0.13.

### 3.2.3. DNRA

DNRA rates ranged from 0 to  $2.6 \mu\text{mol N m}^{-2} \text{h}^{-1}$  for the whole NRE (Figure 5c). There were two centrally located yet separate areas where DNRA rates were elevated by 10 times relative to upstream and downstream values. The high DNRA zone upstream corresponded to high sulfide, but the more seaward high DNRA zone did not. The lowest DNRA rates were measured in the southernmost one third of the NRE where sulfide was lowest, and in both of the two upper branches; one of which (NW branch) was OC rich, while the other (NE branch) was not. On the whole estuary scale, denitrification accounted for 91% of the total nitrogen reduction, with anammox and DNRA accounting for 3.5% and 5.5%, respectively (Figures 5d–5f). However, 17 of the stations, representing approximately one third of the total NRE area had DNRA rates that were 20% or more of the denitrification rate. At the three sites with the highest DNRA rates, this reaction exceeded denitrification by fourfold to fivefold.

## 3.3. Patterns and Covariance Between Geochemistry and N-Cycling Rates

The relationship between the N-cycling rates and two potentially dominant sediment controls, sediment organic carbon (OC) and sulfide, was examined for all stations. Further analysis separately considered the upper NRE where terrestrial OC was prevalent and the lower NRE where OC of marine origin was more common. The relationship between sediment OC and N-cycling rates was nonlinear for all the reactions. When the whole data set was examined, an apparent maximum in rates occurred at 2–4%, 2–4%, and 3–5% OC, for denitrification, anammox, and DNRA, respectively (Figures 6a, 6c, and 6e). Further, when the upper and lower NRE were considered separately, there appeared to be unique and different maxima for denitrification and at 4% OC in the upper NRE and 2% OC in the lower NRE. Despite these apparent %OC-denitrification optima, the overall distribution of %OC yielded a negative correlation with denitrification regardless of position in the NRE (Figure 7). Anammox was strongly correlated to denitrification and followed a similar pattern with respect to an apparent optimum %OC (Figures 6c, 6d, and 7). DNRA, however, increased with rising %OC when %OC was below 3.5, but decreased  $\text{OC} > 4.5$ . The OC % that corresponded to the “breakpoint” between a positive versus negative correlation between DNRA and OC existed roughly at the demarcation between upper and lower NRE (Figure 6e). Regardless of position in the estuary, denitrification and anammox rates decreased, and DNRA increased with higher sulfide concentrations (Figures 6b, 6d, and 6f—see correlation results below).

Pearson’s correlation matrices were used to assess covariance among rates and all sediment geochemical parameters measured. Three separate analyses were conducted. One correlation matrix was generated using

The upper NRE yielded denitrification rates of  $0.33$  to  $62 \mu\text{mol N m}^{-2} \text{h}^{-1}$ . Elevated denitrification was measured in the upper NE, but not in portions of the upper NW branch of the NRE where sulfide was highest. Denitrification rates in the lower NRE ranged from  $1.3$  to  $107 \mu\text{mol N m}^{-2} \text{h}^{-1}$ . There was a small zone of elevated rates along the northern margin of the recently deceased grassbed, but the broadest zone of higher denitrification occurred throughout the lower one third of the NRE where sulfide was uniformly lowest (Figure 5a).

### 3.2.2. Anammox

Anammox ranged from 0 to  $3.1 \mu\text{mol N m}^{-2} \text{h}^{-1}$  for the estuary (Figure 5b). The upper estuary contained anammox rates of 0.0 to  $2.8 \mu\text{mol N m}^{-2} \text{h}^{-1}$ , while the lower NRE had anammox rates ranging from 0.0 to

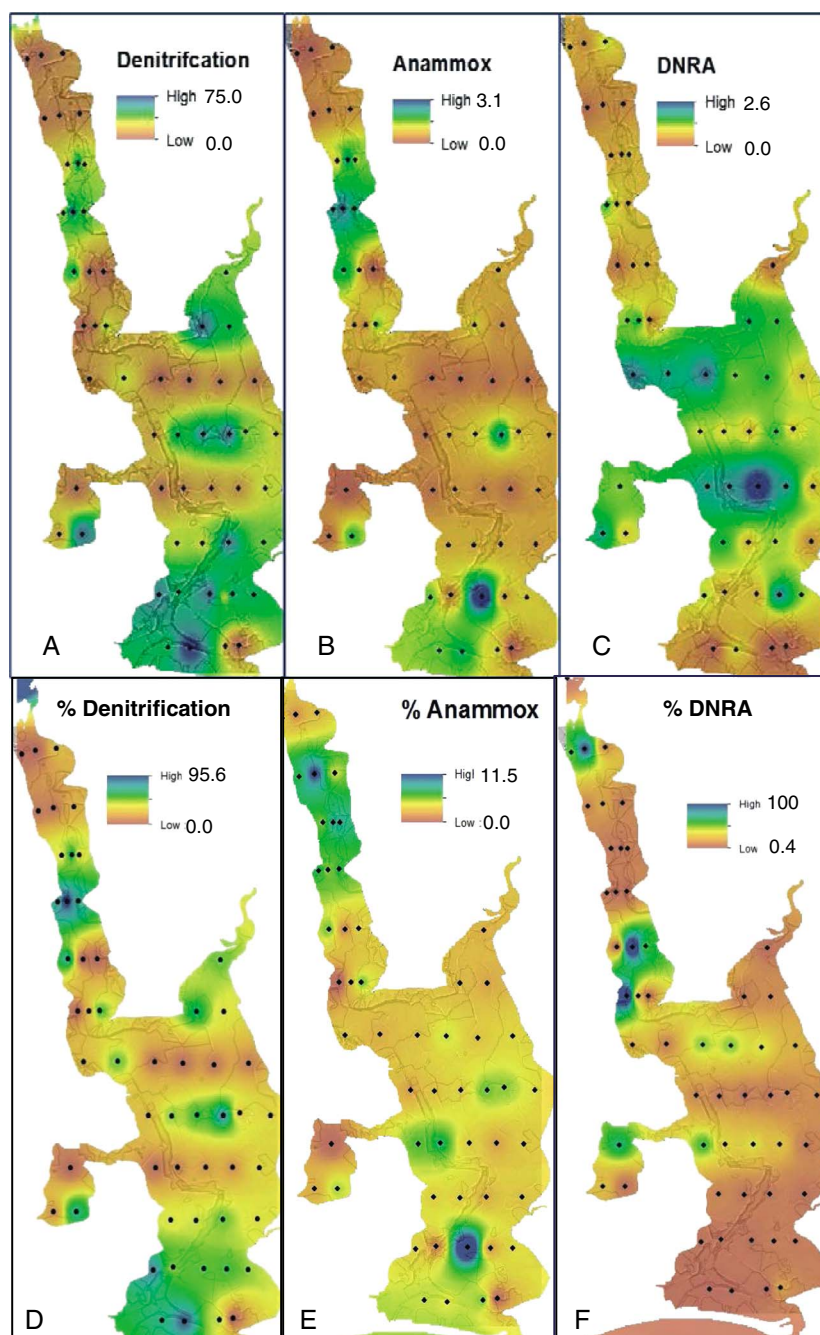


**Figure 5.** (a–c) Microbial rates ( $\mu\text{mol N m}^{-2} \text{h}^{-1}$ ) and (d–f) fractional contribution of each reaction to total  $\text{NO}_x$  respiration within the NRE. Percent contribution by each reaction =  $\text{Rxn}_i / \sum \text{Rxn}_s \times 100$ .

the whole data set from the NRE, while two others were done using data collected above and below the natural geomorphological divide in the NRE (the sandbar separating the upper and lower estuaries; Figures 7a–7c). Data within the correlation tables were color coded according to the absolute value of the correlation coefficients  $|r|$ , where  $|r| > 0.50$  are red,  $0.50 > |r| > 0.40$  are yellow, and  $0.40 > |r| > 0.30$  are green. For the purpose of subsequent discussion, we considered a  $|r| < 0.35$  as a “weak” relationship between parameters regardless of the significance ( $p$  value) as determined by the  $T$  statistic. All but a few comparisons yielded significant relationships ( $p < 0.01$ ) between parameters due to the large number of stations

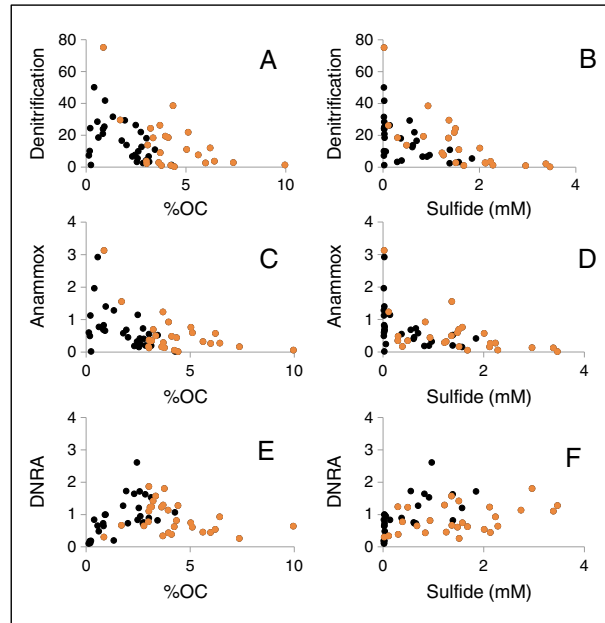


**Figure 6.** Distribution of N reduction rates ( $\mu\text{mol N m}^{-2} \text{h}^{-1}$ ) as a function of (a, c, e) %OC and (b, d, f) pore water sulfide. Upper NRE (orange) and lower NRE (black). Correlation statistics for upper, lower, and all NRE stations are shown in Figure 7.

(Figures 7a–7c) indicating a high degree of covariance among measured values. However, only four correlations yielded a  $|r|$  value above 0.63 (corresponding to a linear regression  $r^2 > 0.40$ ), indicating high scatter among measured values and/or large deviations from linear relationships between parameters.

**3.3.1. Upper Estuary**

In the upper NRE, sulfide and benthic chlorophyll *a* negatively covaried with denitrification, while bulk density exhibited a positive covariance. Anammox exhibited the same relationships as denitrification, as well as a negative covariance with phaeopigments. DNRA covaried positively with extractable ammonium and negatively with %OC.

**3.3.2. Lower Estuary**

In the lower NRE, denitrification rates were inversely correlated to %OC, sediment  $\delta^{13}\text{C}$ , and bulk density. Anammox again exhibited the same relationships as denitrification. DNRA in the lower NRE was strongly positively correlated

with  $\text{NH}_4^+$  concentration, %OC, sediment  $\delta^{15}\text{N}$ , and sulfide, but inversely correlated to chlorophyll *a* and bulk density.

**3.3.3. Whole Estuary**

When considering all stations across the entire estuary, denitrification was positively correlated to bulk density and was negatively correlated to pore water ammonium concentration, %OC, and sulfide. DNRA was positively correlated to pore water ammonium, porosity, and sulfide, but negatively correlated to

A				B				C			
	DNF	ANA	DNRA		DNF	ANA	DNRA		DNF	ANA	DNRA
DNF	1.00			DNF	1.00			DNF	1.00		
ANA	0.85	1.00		ANA	0.97	1.00		ANA	0.78	1.00	
DNRA	-0.14	-0.20	1.00	DNRA	0.11	0.08	1.00	DNRA	-0.24	-0.28	1.00
A:D	-0.10	0.36	-0.15	A:D	-0.21	-0.02	-0.35	A:D	-0.12	0.45	-0.03
Sulfide	-0.41	-0.30	0.33	Sulfide	-0.49	-0.43	0.21	Sulfide	-0.32	-0.26	0.59
Ferrous	0.14	0.15	-0.03	$\rho$	0.46	0.47	0.17	Ferrous	0.15	0.20	-0.10
$\rho$	0.36	0.32	-0.20	$\phi$	-0.31	-0.33	-0.12	$\rho$	0.39	0.42	-0.52
$\phi$	-0.30	-0.27	0.38	Chl-a	-0.45	-0.47	-0.26	$\phi$	-0.31	-0.37	0.73
Chl-a	-0.03	-0.06	-0.33	Phaeo	-0.24	-0.36	0.28	Chl-a	-0.11	-0.06	-0.62
Phaeo	-0.02	-0.14	0.32	$\text{NH}_4^+$	-0.27	-0.26	0.50	Phaeo	0.00	-0.01	0.24
$\text{NH}_4^+$	-0.35	-0.30	0.54	$\delta^{15}\text{N}$	0.16	0.15	0.20	$\text{NH}_4^+$	-0.30	-0.31	0.74
$\delta^{15}\text{N}$	-0.06	-0.11	0.34	$\delta^{13}\text{C}$	0.25	0.21	0.21	$\delta^{15}\text{N}$	-0.31	-0.34	0.57
$\delta^{13}\text{C}$	-0.15	-0.21	0.12	C:N	-0.06	-0.07	-0.13	$\delta^{13}\text{C}$	-0.58	-0.51	-0.23
C:N	0.25	0.02	-0.02	% org	-0.34	-0.33	-0.32	C:N	0.33	0.04	-0.02
% org	-0.35	-0.26	-0.02					% org	-0.44	-0.41	0.62

**Figure 7.** Pearson's correlations between rates and sediment geochemical parameters for (a) entire NRE, (b) upper NRE, and (c) lower NRE. Green, yellow, and red shadings denote the absolute value of the correlation coefficient ( $|r|$ ):  $0.30 < \text{green} < 0.40$ ,  $0.40 < \text{yellow} < 0.50$ , and red  $> 0.50$ .

chlorophyll *a*. Anammox was not correlated to any parameter with a  $|r| > 0.36$ . Comparisons among rates throughout the NRE showed that denitrification was strongly correlated to anammox, but not to DNRA.

Comparison of the correlation matrices (upper versus lower versus entire estuary) revealed that the highest correlation coefficients between rates and selected environmental parameters (e.g., sulfide, chlorophyll *a*, DO, and bulk density) in the upper NRE existed for denitrification and anammox but not for DNRA (red and yellow cells in Figure 7b). In contrast the highest correlation coefficients between rates and selected environmental parameters (e.g., sulfide, chlorophyll *a*, bulk density, porosity  $\text{NH}_4^+$ , and % org) in the lower NRE existed for DNRA, but not for denitrification or anammox (red and yellow cells in Figure 7c). Because the patterns of correlation between different parameters and different reactions was both reaction and location (upper versus lower) dependent, when all data were used (Figure 7a), very few strong correlations among rates and environmental parameters could be identified. In other words the connections between rates and potential environmental controls across the whole estuary were confounded because of apparent differential controls on different rates up versus down estuary as well as by the nonlinear rate versus %OC relationships throughout the NRE.

## 4. Discussion

The NRE sediments were characterized by a varied spatial distribution of carbon abundance and source. All sediments were exposed to uniformly low nitrate in overlying water regardless of position in the estuary, and widespread euryhaline conditions provided ample sulfate for sulfate reduction at all locations. Our experiments did not address the role of photoautotrophs in N retention, which can be diurnally important in these kinds of shallow systems, but instead focused on fates for  $\text{NO}_x$  (denitrification, DNRA, and anammox) which are present in both photic and aphotic settings. Since incubations were performed in the dark, rates are most applicable to nighttime conditions in photic sediments (~35% of our stations) and at all times in sediments where light penetration is  $< 1\%$  of incident (~65% of our stations). The high spatial resolution of our measurements revealed an interactive effect of C load, C source, and sulfide influencing the distribution/magnitude of denitrification, anammox, DNRA, and the resultant degree of N retention in sediments.

### 4.1. Denitrification

On the whole estuary scale, sediment N passing through the  $\text{NO}_{3+2}^-$  pool was primarily exported out of the system via denitrification. Denitrification rates were in line with other temperate estuaries and habitat type [Brin *et al.*, 2014; Joye and Anderson, 2008; Nicholls and Trimmer, 2009; Piehler and Smyth, 2011], accounting for an average of 90% of the total N reduction. Sulfide and carbon exhibited a negative relationship to denitrification rates. The inverse relationship between denitrification and sulfide was encountered throughout the estuary (Figures 6b and 7a–7c) and was consistent with reports of with sulfide inhibition [An and Gardner, 2002; Sørensen *et al.*, 1987]. The sulfide concentrations of 1 to 3 mM found in 20 of NRE sites are similar to sulfide concentrations that inhibited denitrification in other marine studies [Senga *et al.*, 2006]; denitrification in the NRE was effectively absent at sulfide concentrations above 2.2 mM. The largest variations in denitrification rate occurred among sites without sulfide, suggesting that denitrification in areas of low sulfide were controlled by other factors. An inverse relationship between denitrification and OC abundance was observed across all sampling stations, but this covariance masked a more subtle pattern characterized by an optimum OC for denitrification (and possibly for anammox). This observed pattern in the NRE was similar to results of a cross-system comparison that showed a denitrification maximum at intermediate levels of carbon respiration in sediments [Eyre and Ferguson, 2009], but the explanation for the optima in the NRE must be different (Figure 6a). Eyre and Ferguson [2009] attributed higher denitrification at low carbon respiration rates to an increasing supply of N available for coupled nitrification denitrification. The lower denitrification at high carbon respiration rates (i.e., high OC loads) was attributed to loss of sediment faunal communities and extant decreased oxic microzones necessary for coupled nitrification denitrification. But in the NRE, our experiments normalized for sediment structure,  $\text{NO}_x$  and  $\text{O}_2$  supply, were void of macrofauna, and effectively excluded coupled nitrification/denitrification. So the pattern observed in the NRE must be attributable to some other reaction scale factor that is related to geochemical controls other than  $\text{O}_2$  and  $\text{NO}_x$ . We surmise that it arises from some interactive effect of OC load, its lability, and the negative effect of sulfide on denitrification. The existence of two optima %OC for denitrification, one at lower OC concentration in the lower NRE where OC was marine derived and a higher OC concentration for the upper NRE where

the OC was terrestrially derived, suggests that OC lability plays a role (Figure 6a). The shape of the denitrification versus OC distribution was the same for upper and lower NRE, but the optimum OC concentration was shifted higher for the presumably less labile terrestrial OC. The interaction between OC load/lability and sulfate reduction may provide a further control on denitrification. When the total amounts of OC exceed the OC-type-specific optima, sulfate reduction (fueled by  $\sim 20$  mM  $\text{SO}_4^{2-}$  concentrations in overlying water) yielded higher pore water sulfide concentration that suppressed denitrification and caused the observed negative covariance between denitrification and sulfide regardless of position in the estuary (Figures 4, 6b, and 7a–7c). Sulfide enhancement of DNRA competing with denitrification for  $\text{NO}_x$  may have added a secondary suppression of denitrification at high OC high sulfide concentrations (discussed below).

#### 4.2. Anammox

The anammox contribution to total N reduction (0–11%) in the NRE was expectedly small relative to open ocean oxygen minimum zones and other low OC systems [Devol, 2003; Engström *et al.*, 2009; Kuypers *et al.*, 2005; Ward *et al.*, 2008]. The low rates in the NRE were typical for this type of temperate coastal sediment with moderate amounts of OC and in line with anammox rates and anammox:denitrification ratios reported for similar systems [Brin *et al.*, 2014; Dale *et al.*, 2009; Dalsgaard *et al.*, 2005; Rich *et al.*, 2008]. Within the estuary, anammox and denitrification were highly correlated. Similar to denitrification, there also appeared to be two optima OC concentrations for anammox superimposed against a generally negative covariance between anammox with OC and sulfide (Figures 6c, 6d, and 7a–7c). The observed higher anammox rates in low OC sediments would be consistent with lab, modeling, and field studies [Algar and Vallino, 2014; Engström *et al.*, 2005] that indicate more favorable anammox conditions at low OC. The negative covariance between anammox and sulfide in the NRE matches a similar negative sulfide effect reported by Jensen *et al.* [2008] but contradicts studies that report a positive relationship between sulfide and anammox [Lisa *et al.*, 2014; Wenk *et al.*, 2013]. The anammox enhancement by sulfide in these studies was attributed to higher  $\text{NH}_4^+$  delivery to anammox by sulfate reduction and/or by DNRA that was favored at high sulfide levels. There was a negative correlation between anammox and  $\text{NH}_4^+$  (Figures 8a–8c) in the NRE, but the threefold to tenfold higher sulfide in the NRE, relative to sediments reported by Lisa *et al.* [2014], may limit anammox in the NRE by blocking  $\text{NO}_2^-$  supply from nitrification [Hines *et al.*, 2013] and/or denitrification. Unlike, Kartal *et al.* [2007] and Lisa *et al.* [2014], there was no correlative evidence to suggest that DNRA was coupled to anammox in the NRE.

#### 4.3. DNRA

The range of DNRA rates measured within the NRE spans rates reported across a wide variety of coastal systems (reviewed by Giblin *et al.* [2013]). In terms of the importance of DNRA relative to denitrification, the highest DNRA:denitrification ratio of 3:1 in the NRE was similar to some of the highest ratios measured in warm sulfide-rich systems [An and Gardner, 2002], but overall, the estuarine-averaged DNRA:denitrification ratio of 1:5 was more typical for reported values in all but the most organic-rich aquaculture settings [Christensen *et al.*, 2000]. The spatial variation in the DNRA rate appeared to be largely independent of the denitrification and anammox N removal pathways. This decoupling of N removal reactions from N retention suggests that geochemical controls within the NRE affect DNRA and denitrification/anammox differently.

The sulfide and carbon relationships to DNRA rates may indicate two modes of DNRA within the NRE, and/or some underlying role of carbon source dependent upon position in the estuary. High concentrations of sulfide are known to promote autotrophic DNRA [An and Gardner, 2002; Senga *et al.*, 2006]. Data from the NRE, in general, support this mechanism; however, there is less evidence for this DNRA pathway in the upper NW branch (Figure 6f). While there were positive correlations between sulfide and DNRA in the upper and lower NRE, OC abundance was positively correlated with DNRA in only the lower NRE where the carbon source was more marine in origin (Figures 6f and 8c). When all data were considered, there was a single optimum OC% for DNRA across all stations, but unlike denitrification, there was no indication that there were separate optima unique to position in the estuary or OC source type. The negative relationship between DNRA and OC in the upper estuary was unexpected (Figure 6e). The upper NRE has the highest concentrations of organic matter within the estuary, yet the area-averaged DNRA rate in the upper NRE was only two thirds of the DNRA in the rest of the estuary. These different DNRA-OC-sulfide relationships in the upper and lower NRE could be due to switching DNRA modes between sulfide-driven chemoautotrophy in the upper NRE to fermentative pathways in the lower NRE, perhaps in response to the spatial differences in carbon quality. As similarly reported for other anaerobic respiratory pathways [Hee *et al.*, 2001], the

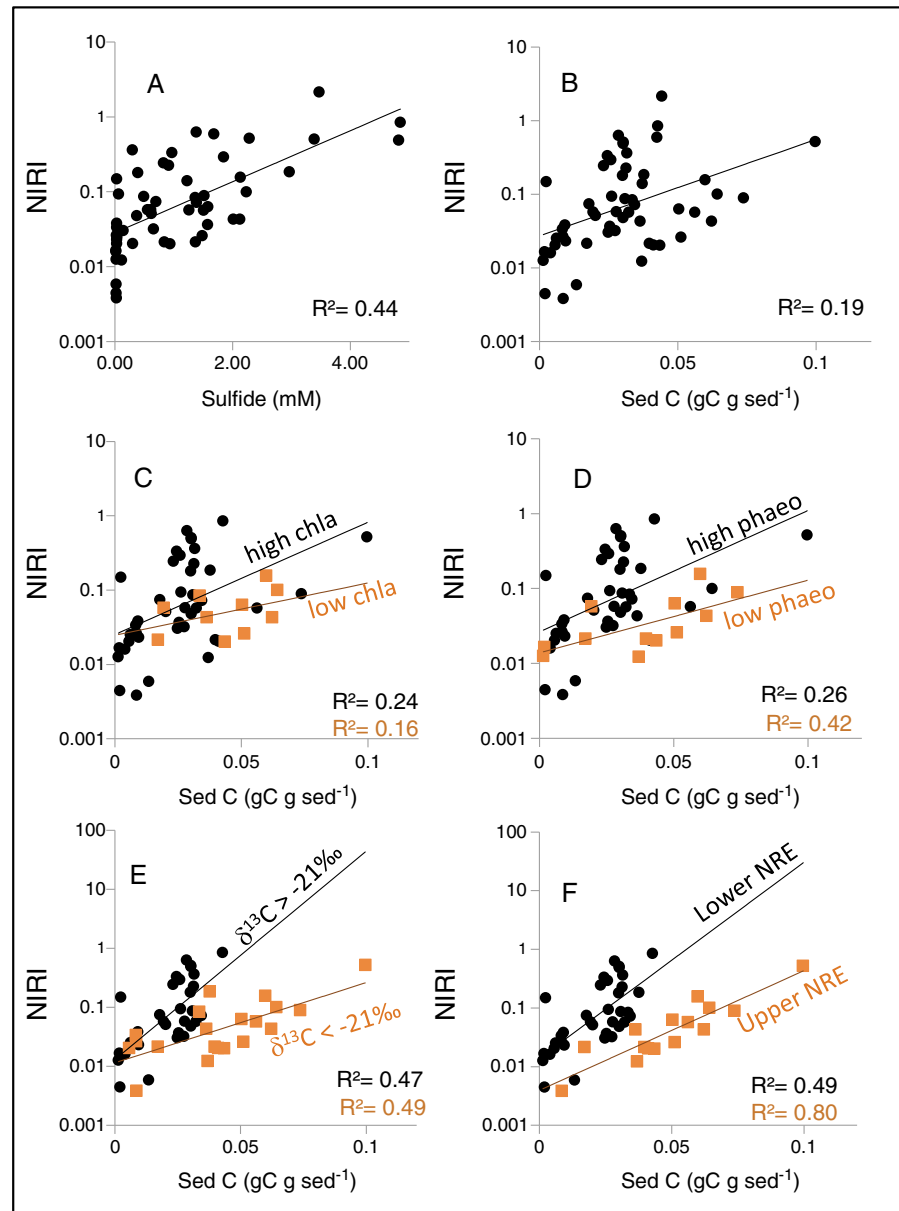


**Figure 8.** Nitrogen Retention Index (NIRI) as a function of (a) sulfide and (b) OC using all data and as a function of OC after binning data by (c) chlorophyll *a*, (d) phaeopigments, and (e)  $\delta^{13}\text{C}$ , and by location in the (f) NRE. Symbols and regression parameters in black denote values for the higher range of the binned data in Figures 8c–8e or the upper NRE in Figure 8f. Threshold values for binning data were chlorophyll *a* = 0.5  $\mu\text{g chlorophyll } a \text{ g}^{-1}$ , phaeopigments = 3  $\mu\text{g phaeo g}^{-1}$ , and  $\delta^{13}\text{C} = -21\text{‰}$  for Figures 8c–8e, and above and below the sandbar for Figure 8f. All panels:  $n = 54$ .

thermodynamic favorability of the fermentative versus autotrophic DNRA pathways would be affected by carbon source. Rates of both denitrification [Lu et al., 2009; Sirivedhin and Gray, 2006] and DNRA [Yin et al., 2002] are known to vary with different carbon source and/or age with a drop in rates of both DNRA and denitrification observed in sediments with older more refractory carbon [Tobias et al., 2001]. The same high sulfide conditions at the highest OC concentrations that we suggest suppressed denitrification would favor a DNRA switch from a low lability OC source of electrons to the more readily available sulfide source. By extension, at lower sulfide concentrations (e.g., less than 2 mM), the denitrification rate would be more closely tied to OC lability (hence the occurrence of OC-type-specific %OC optima for denitrification) than DNRA because of the lessened ability of most denitrifiers to switch to a non-OC reductant.

#### 4.4. Nitrogen Retention Index

When all three reaction rates are collapsed into a single Nitrogen Retention Index ( $\text{NIRI} = \text{DNRA}/(\text{denitrification} + \text{anammox})$ ) the data support the proposition that OC availability is an important determinant of N retention versus loss by influencing the proportion of denitrification, anammox, and DNRA processing of DIN as described by *Algar and Vallino* [2014]. The NRE data also indicate that there may be further, and equally important, controls exerted by sulfide and OC source type. NIRI was tightly correlated to sulfide which accounted for 44% of its variance throughout the NRE (Figure 8a). Given the covariance between sulfide and OC, it is difficult, however, to deconstruct OC versus sulfide effects on NIRI. While NIRI was also significantly correlated to OC, the sediment OC accounted for less than 19% of the variance in NIRI across the whole estuary (Figure 8b). We attribute this weaker correlation between NIRI and OC to differences in carbon source (i.e., lability). To assess this possibility, we grouped the stations according to ranges in some of the various organic matter characteristics measured. The assumption here was that similar carbon sources have similar lability and also display similar organic matter source metrics like  $\delta^{13}\text{C}$ , chlorophyll *a*, and phaeopigments. When the data are binned by these various organic matter source metrics to try to account for difference in lability (e.g.,  $\delta^{13}\text{C}$ , chlorophyll *a*, and phaeopigments), stronger relationships between OC abundance and NIRI were achieved (Figures 8c–8e). For example, when data were split into two groups according to  $\delta^{13}\text{C}$  (greater or less than  $-21\text{‰}$  used to separate marine versus terrestrial OC), the OC abundance became a much stronger predictor of NIRI for each set of data ( $R^2 = 0.47\text{--}0.49$ ) relative to the entire data set ( $R^2 = 0.19$ ; Figure 8c). The regression slope in Figure 8c was steeper for the marine-derived OC, suggesting greater NIRI response to that OC source relative to similar changes in terrestrial OC abundance. Similar but a less improved OC versus NIRI correlation was achieved by considering chlorophyll *a* (an indication of recent phytoplankton carbon) above and below  $0.4\ \mu\text{g chlorophyll } a\ \text{g sediment}^{-1}$ , and with phaeopigments (an indication of recently degraded autotrophic biomass) above and below  $0.3\ \mu\text{g phaeo g sediment}^{-1}$  (Figures 8d and 8e). We suggest that this binning of the data by carbon source metric, in part, normalizes for C lability. No improvement in the NIRI versus OC abundance was seen when data were binned by C:N ratio, likely because C:N had two maxima from two different sources—terrestrial and sea grass which may differ in lability. In the estuary, the distribution of the  $\delta^{13}\text{C}$ , chlorophyll *a*, and phaeopigment was divided spatially roughly at the sandbar whereby parsing the data into upper and lower estuary bins similarly enhanced the correlation between OC and NIRI (Figure 8f).

Since most coastal sediments are of mixed carbon source, there is no way to know a priori what carbon metrics, thresholds, or spatial boundaries are best used to bin data for the purpose of relating OC to NIRI. So when all data were considered (across the upper and lower NRE and regardless of carbon source metric), sulfide emerged as the single best predictor of NIRI—explaining 44% of its variance throughout the entire NRE (Figure 8a). As a predictor of NIRI, we suggest that in marine and mesoeuryhaline estuarine settings (i.e., ample  $\text{SO}_4^{-2}$  supply), the pore water sulfide provides an integrated measure of OC availability (abundance and lability). Further, the sulfide measurement incorporates any potentially inhibitory sulfide effects on denitrification or enhancements of DNRA with its extant influence on NIRI. We suggest that as a single metric, sulfide may have utility as a proxy for gauging the distribution of denitrification, anammox, and DNRA that controls N retention versus loss.

An alternative explanation of the distribution of denitrification, anammox, and DNRA and NIRI is one of  $\text{NO}_{3+2}^-$  control. It is possible that the differences in upper and lower NRE were more indicative of higher inputs of nitrate rather than carbon source/lability differences. The lower slope NIRI versus OC regression in the lower estuary compared to the upper estuary would be consistent with *Algar and Vallino* [2014] that show denitrification and anammox were favored over DNRA at higher  $\text{NO}_{3+2}^-$  to OC ratios provided that there actually was more  $\text{NO}_{3+2}^-$  in situ in the upper NRE. But we measured uniformly low  $\text{NO}_{3+2}^-$  everywhere in the estuary, with no evidence of gradient along the estuarine axis. Although characterization of the in situ  $\text{NO}_{3+2}^-$  supply (i.e., the production rate of  $\text{NO}_{3+2}^-$ ) was not resolvable with the existing data, it seems unlikely that  $\text{NO}_{3+2}^-$  availability was the single cause of the observed NIRI distribution, particularly after considering that rates were determined under experimentally standardized  $\text{NO}_2^-$  additions. For that to be so, there would have been undetected differential  $\text{NO}_{3+2}^-$  inputs in each of the upper branches of the NRE, and from tidal flooding waters (to acct for higher denitrification in the lower NRE), and the effects of sulfide would have to be ignored, as well as discounting the different carbon sources in the upper versus

lower NRE. The ability to resolve in situ  $\text{NO}_{3+2}^-$  availability across a spectrum of OC abundances and labilities seems essential for assessing whether the OC: $\text{NO}_{3+2}^-$  ratio controls on nitrate/nitrite respiration observed in the lab and in models [Algar and Vallino, 2014; Kraft et al., 2014b] translate directly to an altered NRI in the field, or whether, as we suggest, the OC source and sulfide are important coregulators.

#### Acknowledgments

The contents of this work are solely the responsibility of the authors and do not necessarily represent the views of the U.S. Coast Guard or the Federal Government. This work was supported by the Connecticut Sea Grant. Anyone wishing to collaborate on use of the data analyzed here should contact Patrick Plummer (Patrick.plummer@uscga.edu) with the request.

#### References

- Algar, C., and J. Vallino (2014), Predicting microbial nitrate reduction pathways in coastal sediments, *Aquat. Microb. Ecol.*, *71*(3), 223–238, doi:10.3354/ame01678.
- Aminot, A., and F. Rey (2000), Standard procedure for the determination of chlorophyll *a* by spectroscopic methods, pp. 7–10, Int. Council for the Explor. of the Sea.
- An, S., and W. Gardner (2002), Dissimilatory nitrate reduction to ammonium (DNRA) as a nitrogen link, versus denitrification as a sink in a shallow estuary (Laguna Madre/Baffin Bay, Texas), *Mar. Ecol. Prog. Ser.*, *237*, 41–50, doi:10.3354/meps237041.
- Babbin, A. R., and B. B. Ward (2013), Controls on nitrogen loss processes in Chesapeake Bay sediments, *Environ. Sci. Technol.*, *47*(9), 4189–4196, doi:10.1021/es304842r.
- Babbin, A. R., R. G. Keil, A. H. Devol, and B. B. Ward (2014), Organic matter stoichiometry, flux, and oxygen control nitrogen loss in the ocean, *Science*, *344*(6182), 406–408, doi:10.1126/science.1248364.
- Bianchi, T. S., and E. A. Canuel (2011), *Chemical Biomarkers in Aquatic Ecosystems*, Princeton Univ. Press, Princeton, N. J., doi:10.1515/9781400839100.
- Braman, R. S., and S. A. Hendrix (1989), Nanogram nitrite and nitrate determination in environmental and biological materials by vanadium (III) reduction with chemiluminescence detection, *Anal. Chem.*, *61*(24), 2715–2718, doi:10.1021/ac00199a007.
- Brandes, J. A., A. H. Devol, and C. Deutsch (2007), New developments in the marine nitrogen cycle, *ChemInform*, *38*(20), doi:10.1002/chin.200720269.
- Brin, L. D., A. E. Giblin, and J. J. Rich (2014), Environmental controls of anammox and denitrification in southern New England estuarine and shelf sediments, *Limnol. Oceanogr.*, *59*(3), 851–860, doi:10.4319/lo.2014.59.3.0851.
- Brunet, R. C., and L. J. Garcia-Gil (1996), Sulfide-induced dissimilatory nitrate reduction to ammonia in anaerobic freshwater sediments, *FEMS Microbiol. Ecol.*, *21*(2), 131–138, doi:10.1111/j.1574-6941.1996.tb00340.x.
- Burgin, A. J., and S. K. Hamilton (2007), Have we overemphasized the role of denitrification in aquatic ecosystems? A review of nitrate removal pathways, *Front. Ecol. Environ.*, *5*, 89–96, doi:10.1890/1540-9295(2007)5[89:HWOTRO]2.0.CO;2.
- Burgin, A. J., and S. K. Hamilton (2008),  $\text{NO}_3^-$ -driven  $\text{SO}_4^{2-}$  production in freshwater ecosystems: Implications for N and S cycling, *Ecosystems*, *11*(6), 908–922, doi:10.1007/s10021-008-9169-5.
- Caffrey, J., N. P. Sloth, H. F. Kaspar, and T. H. Blackburn (1993), Effect of organic loading on nitrification and denitrification in a marine sediment microcosm, *FEMS Microbiol. Ecol.*, *12*(3), 159–167, doi:10.1016/0168-6496(93)90011-u.
- Canfield, D. E., F. J. Stewart, B. Thamdrup, L. De Brabandere, T. Dalsgaard, E. F. Delong, N. P. Revsbech, and O. Ulloa (2010), A cryptic sulfur cycle in oxygen-minimum-zone waters off the Chilean coast, *Science*, *330*(6009), 1375–1378, doi:10.1126/science.1196889.
- Christensen, P., S. Rysgaard, N. Sloth, T. Dalsgaard, and S. Schwærter (2000), Sediment mineralization, nutrient fluxes, denitrification and dissimilatory nitrate reduction to ammonium in an estuarine fjord with sea cage trout farms, *Aquat. Microb. Ecol.*, *21*, 73–84, doi:10.3354/ame021073.
- Cline, J. D. (1969), Spectrophotometric determination of hydrogen sulfide in natural waters, *Limnol. Oceanogr.*, *14*(3), 454–458, doi:10.4319/lo.1969.14.3.0454.
- Cornwell, J. C., W. M. Kemp, and T. M. Kana (1999), Denitrification in coastal ecosystems: Methods, environmental controls, and ecosystem level controls, a review, *Aquat. Ecol.*, *33*, 41–54, doi:10.1023/a:1009921414151.
- Crowe, S. A., D. E. Canfield, A. Mucci, B. Sundby, and R. Maranger (2012), Anammox, denitrification and fixed-nitrogen removal in sediments from the Lower St. Lawrence Estuary, *Biogeosciences*, *9*(11), 4309–4321, doi:10.5194/bg-9-4309-2012.
- Dale, O. R., C. R. Tobias, and B. Song (2009), Biogeographical distribution of diverse anaerobic ammonium oxidizing (anammox) bacteria in Cape Fear River Estuary, *Environ. Microbiol.*, *11*(5), 1194–1207, doi:10.1111/j.1462-2920.2008.01850.x.
- Dalsgaard, T., D. E. Canfield, J. Petersen, B. Thamdrup, and J. Acuña-González (2003),  $\text{N}_2$  production by the anammox reaction in the anoxic water column of Golfo Dulce, Costa Rica, *Nature*, *422*(6932), 606–608, doi:10.1038/nature01526.
- Dalsgaard, T., B. Thamdrup, and D. E. Canfield (2005), Anaerobic ammonium oxidation (anammox) in the marine environment, *Res. Microbiol.*, *156*(4), 457–464, doi:10.1016/j.resmic.2005.01.011.
- Devol, A. H. (2003), Nitrogen cycle: Solution to a marine mystery, *Nature*, *422*(6932), 575–576, doi:10.1038/422575a.
- Dong, L. F., M. Naqasima Sobey, C. J. Smith, I. Rusmana, W. Phillips, A. Stott, A. Mark Osborn, and D. B. Nedwell (2011), Dissimilatory reduction of nitrate to ammonium, not denitrification or anammox, dominates benthic nitrate reduction in tropical estuaries, *Limnol. Oceanogr.*, *56*(1), 279–291, doi:10.4319/lo.2011.56.1.0279.
- Engström, P., T. Dalsgaard, S. Hulth, and R. C. Aller (2005), Anaerobic ammonium oxidation by nitrite (anammox): Implications for  $\text{N}_2$  production in coastal marine sediments, *Geochim. Cosmochim. Acta*, *69*(8), 2057–2065, doi:10.1016/j.gca.2004.09.032.
- Engström, P., C. R. Penton, and A. H. Devola (2009), Anaerobic ammonium oxidation in deep-sea sediments off the Washington margin, *Limnol. Oceanogr.*, *54*(5), 1643–1652, doi:10.4319/lo.2009.54.5.1643.
- Eyre, B. D., and A. J. P. Ferguson (2009), Denitrification efficiency for defining critical loads of carbon in shallow coastal ecosystems, in *Eutrophication in Coastal Ecosystems*, *Hydrobiologia*, vol. 629, pp. 137–146, Springer, Dordrecht, Netherlands, doi:10.1007/978-90-481-3385-7\_12.
- Fulweiler, R. W., S. W. Nixon, B. A. Buckley, and S. L. Granger (2007), Reversal of net dinitrogen gas flux in coastal marine sediments, *Nature*, *448*, 180–182, doi:10.1038/nature05963.
- Gardner, W. S., M. J. McCarthy, S. An, D. Sobolev, K. S. Sell, and D. Brock (2006), Nitrogen fixation and dissimilatory nitrate reduction to ammonium (DNRA) support nitrogen dynamics in Texas estuaries, *Limnol. Oceanogr.*, *51*, 558–568, doi:10.4319/lo.2006.51.1\_part\_2.0558.
- Giblin, A., C. Tobias, B. Song, N. Weston, G. Banta, and V. Rivera-Monroy (2013), The importance of dissimilatory nitrate reduction to ammonium (DNRA) in the nitrogen cycle of coastal ecosystems, *Oceanography*, *26*(3), 124–131, doi:10.5670/oceanog.2013.54.
- Glud, R. N., B. Thamdrup, H. Stahl, F. Wenzhoefer, A. Glud, H. Nomaki, K. Oguri, N. P. Revsbech, and H. Kitazato (2009), Nitrogen cycling in a deep ocean margin sediment (Sagami Bay, Japan), *Limnol. Oceanogr.*, *54*(3), 723–734, doi:10.4319/lo.2009.54.3.0723.

- Hee, C. A., T. K. Pease, M. J. Alperin, and C. S. Martens (2001), Dissolved organic carbon production and consumption in anoxic marine sediments: A pulsed-tracer experiment, *Limnol. Oceanogr.*, *46*(8), 1908–1920, doi:10.4319/lo.2001.46.8.1908.
- Hines, D., J. Lisa, B. Song, C. Tobias, and S. Borrett (2013), Estimating the effects of seawater intrusion on an estuarine nitrogen cycle by comparative network analysis, *Mar. Ecol. Prog. Ser.*, *524*, 137–154, doi:10.3354/meps11187.
- Holmes, R., J. McClelland, D. Sigman, B. Fry, and B. Peterson (1998), Measuring  $15\text{N-NH}_4^+$  in marine, estuarine and fresh waters: An adaptation of the ammonia diffusion method for samples with low ammonium concentrations, *Mar. Chem.*, *60*, 235–243, doi:10.1016/S0304-4203(97)00099-6.
- Jensen, M. M., M. M. M. Kuypers, G. Lavik, and B. Thamdrup (2008), Rates and regulation of anaerobic ammonium oxidation and denitrification in the Black Sea, *Limnol. Oceanogr.*, *53*(1), 23–36, doi:10.4319/lo.2008.53.1.0023.
- Jin, R., G. Yang, J. Yu, and P. Zheng (2012), The inhibition of the Anammox process: A review, *Chem. Eng. J.*, *197*, 67–79, doi:10.1016/j.cej.2012.05.014.
- Joye, S. B., and I. C. Anderson (2008), Nitrogen cycling in coastal sediments, in *Nitrogen in the Marine Environment*, 2nd ed., pp. 867–915, Academic Press, Burlington, Mass., doi:10.1016/b978-0-12-372522-6.00019-0.
- Joye, S. B., and J. T. Hollibaugh (1995), Influence of sulfide inhibition of nitrification on nitrogen regeneration in sediments, *Science*, *270*(5236), 623–625, doi:10.1126/science.270.5236.623.
- Kana, T. M., M. B. Sullivan, J. C. Cornwell, and K. M. Groszkowski (1998), Denitrification in estuarine sediments determined by membrane inlet mass spectrometry, *Limnol. Oceanogr.*, *43*(2), 334–339, doi:10.4319/lo.1998.43.2.0334.
- Kartal, B., M. M. M. Kuypers, G. Lavik, J. Schalk, H. J. M. Op den Camp, M. S. M. Jetten, and M. Strous (2007), Anammox bacteria disguised as denitrifiers: Nitrate reduction to dinitrogen gas via nitrite and ammonium, *Environ. Microbiol.*, *9*(3), 635–642, doi:10.1111/j.1462-2920.2006.01183.x.
- King, D., and D. B. Nedwell (1985), The influence of nitrate concentration upon the end-products of nitrate dissimilation by bacteria in anaerobic salt marsh sediment, *FEMS Microbiol. Lett.*, *31*(1), 23–28, doi:10.1111/j.1574-6968.1985.tb01127.x.
- Kraft, B., H. E. Tegetmeyer, D. Meier, J. S. Geelhoed, and M. Strous (2014a), Rapid succession of uncultured marine bacterial and archaeal populations in a denitrifying continuous culture, *Environ. Microbiol.*, *16*(10), 3275–3286, doi:10.1111/1462-2920.12552.
- Kraft, B., H. E. Tegetmeyer, R. Sharma, M. G. Klotz, T. G. Ferdelman, R. L. Hettich, J. S. Geelhoed, and M. Strous (2014b), The environmental controls that govern the end product of bacterial nitrate respiration, *Science*, *345*(6197), 676–679, doi:10.1126/science.1254070.
- Kuypers, M. M. M., G. Lavik, D. Woebken, M. Schmid, B. M. Fuchs, R. Amann, B. B. Jørgensen, and M. S. M. Jetten (2005), Massive nitrogen loss from the Benguela upwelling system through anaerobic ammonium oxidation, *Proc. Natl. Acad. Sci. U.S.A.*, *102*(18), 6478–6483, doi:10.1073/pnas.0502088102.
- Lisa, J., B. Song, C. Tobias, and K. Duernberger (2014), Impacts of freshwater flushing on anammox community structure and activities in the New River Estuary, USA, *Aquat. Microb. Ecol.*, *72*(1), 17–31, doi:10.3354/ame01682.
- Lu, S., H. Hu, Y. Sun, and J. Yang (2009), Effect of carbon source on the denitrification in constructed wetlands, *J. Environ. Sci.*, *21*(8), 1036–1043, doi:10.1016/S1001-0742(08)62379-7.
- Meyer, R. L., N. Risgaard-Petersen, and D. E. Allen (2005), Correlation between anammox activity and microscale distribution of nitrite in a subtropical mangrove sediment, *Appl. Environ. Microbiol.*, *71*(10), 6142–6149, doi:10.1128/aem.71.10.6142-6149.2005.
- Mohan, S. B., and J. A. Cole (2007), The dissimilatory reduction of nitrate to ammonia by anaerobic bacteria, in *Biology of the Nitrogen Cycle*, pp. 93–106, Elsevier, Amsterdam, Netherlands, doi:10.1016/b978-0-44452857-5.50008-4.
- Nicholls, J., and M. Trimmer (2009), Widespread occurrence of the anammox reaction in estuarine sediments, *Aquat. Microb. Ecol.*, *55*, 105–113, doi:10.3354/ame01285.
- Nielsen, K., L. Nielsen, and P. Rasmussen (1995), Estuarine nitrogen retention independently estimated by the denitrification rate and mass balance methods: A study of Norsminde Fjord, Denmark, *Mar. Ecol. Prog. Ser.*, *119*, 275–283, doi:10.3354/meps119275.
- Piehler, M. F., and A. R. Smyth (2011), Habitat-specific distinctions in estuarine denitrification affect both ecosystem function and services, *Ecosphere*, *2*(1), 12, doi:10.1890/es10-00082.1.
- Rich, J. J., O. R. Dale, B. Song, and B. B. Ward (2008), Anaerobic ammonium oxidation (Anammox) in Chesapeake Bay sediments, *Microb. Ecol.*, *55*(2), 311–320, doi:10.1007/s00248-007-9277-3.
- Seitzinger, S., J. A. Harrison, J. Böhlke, A. Bouwman, R. Lowrance, B. Peterson, C. Tobias, and G. V. Drecht (2006), Denitrification across landscapes and waterscapes: A synthesis, *Ecol. Appl.*, *16*, 2064–2090, doi:10.1890/1051-0761(2006)016[2064:DALAWA]2.0.CO;2.
- Senga, Y., K. Mochida, R. Fukumori, N. Okamoto, and Y. Seike (2006),  $\text{N}_2\text{O}$  accumulation in estuarine and coastal sediments: The influence of  $\text{H}_2\text{S}$  on dissimilatory nitrate reduction, *Estuarine Coastal Shelf Sci.*, *67*(1–2), 231–238, doi:10.1016/j.ecss.2005.11.021.
- Sirivedhin, T., and K. A. Gray (2006), Factors affecting denitrification rates in experimental wetlands: Field and laboratory studies, *Ecol. Eng.*, *26*(2), 167–181, doi:10.1016/j.ecoleng.2005.09.001.
- Smith, P., and K. Bogren (2001), Determination of nitrate and/or nitrite in brackish or seawater by flow injection analysis colorimeter, QuickChem Method 31-107-04-1-E, Methods manual, Lachat Instrum.
- Solorzano, L. (1969), Determination of ammonia in natural waters by the phenol hypochlorite method, *Limnol. Oceanogr.*, *14*(5), 799–801, doi:10.4319/lo.1969.14.5.0799.
- Song, B., and C. R. Tobias (2011), Molecular and stable isotope methods to detect and measure anaerobic ammonium oxidation (anammox) in aquatic ecosystems, in *Research on Nitrification and Related Processes, Part B*, pp. 63–89, Academic Press, San Diego, Calif., doi:10.1016/b978-0-12-386489-5.00003-8.
- Sørensen, J. (1987), Nitrate reduction in marine sediment: Pathways and interactions with iron and sulfur cycling, *Geomicrobiol. J.*, *5*(3–4), 401–421, doi:10.1080/01490458709385976.
- Sørensen, J., L. K. Rasmussen, and I. Koike (1987), Micromolar sulfide concentrations alleviate acetylene blockage of nitrous oxide reduction by denitrifying *Pseudomonas fluorescens*, *Can. J. Microbiol.*, *33*(11), 1001–1005, doi:10.1139/m87-176.
- Stokey, L. L. (1970), Ferrozine—A new spectrophotometric reagent for iron, *Anal. Chem.*, *42*(7), 779–781, doi:10.1021/ac60289a016.
- Thamdrup, B., and T. Dalsgaard (2002), Production of  $\text{N}_2$  through anaerobic ammonium oxidation coupled to nitrate reduction in marine sediments, *Appl. Environ. Microbiol.*, *68*(3), 1312–1318, doi:10.1128/aem.68.3.1312-1318.2002.
- Tiedje, J. (1988), Ecology of denitrification and dissimilatory nitrate reduction to ammonium, in *Biology of Anaerobic Microorganisms*, vol. 717, pp. 179–244, John Wiley, New York.
- Tobias, C., I. Anderson, E. Canuel, and S. Macko (2001), Nitrogen cycling through a fringing marsh-aquifer ecotone, *Mar. Ecol. Prog. Ser.*, *210*, 25–39, doi:10.3354/meps210025.
- Trimmer, M., J. C. Nicholls, and B. Deflandre (2003), Anaerobic ammonium oxidation measured in sediments along the Thames estuary, United Kingdom, *Appl. Environ. Microbiol.*, *69*(11), 6447–6454, doi:10.1128/aem.69.11.6447-6454.2003.

- Trimmer, M., J. C. Nicholls, N. Morley, C. A. Davies, and J. Aldridge (2005), Biphasic behavior of anammox regulated by nitrite and nitrate in an estuarine sediment, *Appl. Environ. Microbiol.*, *71*(4), 1923–1930, doi:10.1128/aem.71.4.1923-1930.2005.
- Tugtas, A. E., and S. G. Pavlostathis (2007), Electron donor effect on nitrate reduction pathway and kinetics in a mixed methanogenic culture, *Biotechnol. Bioeng.*, *98*(4), 756–763, doi:10.1002/bit.21487.
- Ward, B. B., C. B. Tuit, A. Jayakumar, J. J. Rich, J. Moffett, and S. W. A. Naqvi (2008), Organic carbon, and not copper, controls denitrification in oxygen minimum zones of the ocean, *Deep Sea Res., Part I*, *55*(12), 1672–1683, doi:10.1016/j.dsr.2008.07.005.
- Wenk, C. B., J. Blees, J. Zopfi, M. Veronesi, A. Bourbonnais, C. J. Schubert, H. Niemann, and M. F. Lehmann (2013), Anaerobic ammonium oxidation (anammox) bacteria and sulfide-dependent denitrifiers coexist in the water column of a meromictic south-alpine lake, *Limnol. Oceanogr.*, *58*(1), 1–12, doi:10.4319/lo.2013.58.1.0001.
- Yin, S., D. Chen, L. Chen, and R. Edis (2002), Dissimilatory nitrate reduction to ammonium and responsible microorganisms in two Chinese and Australian paddy soils, *Soil Biol. Biochem.*, *34*(8), 1131–1137, doi:10.1016/s0038-0717(02)00049-4.